A DNA-Directed Light-Harvesting/Reaction Center System

ARTICLE *in* JOURNAL OF THE AMERICAN CHEMICAL SOCIETY · OCTOBER 2014

Impact Factor: 12.11 · DOI: 10.1021/ja509018g · Source: PubMed

10 AUTHORS, INCLUDING:

Andrey V. Loskutov
International Genomics Consortium / Paradig…
24 PUBLICATIONS **187** CITATIONS
SEE PROFILE

Yan Liu
Arizona State University
151 PUBLICATIONS **6,644** CITATIONS
SEE PROFILE

Neal W Woodbury
Arizona State University
138 PUBLICATIONS **4,017** CITATIONS
SEE PROFILE

Hao Yan
Arizona State University
150 PUBLICATIONS **10,047** CITATIONS
SEE PROFILE

JACS
JOURNAL OF THE AMERICAN CHEMICAL SOCIETY

Article

pubs.acs.org/JACS

A DNA-Directed Light-Harvesting/Reaction Center System

Palash K. Dutta,[†,‡] Symon Levenberg,[†,‡] Andrey Loskutov,[‡] Daniel Jun,[§] Rafael Saer,[§] J. Thomas Beatty,[§] Su Lin,[†,‡] Yan Liu,[†,‡] Neal W. Woodbury,*[,†,‡] and Hao Yan*[,†,‡]

[†]Department of Chemistry and Biochemistry and [‡]The Biodesign Institute, Arizona State University, Tempe, Arizona 85287, United States

[§]Department of Microbiology and Immunology, University of British Columbia, Vancouver, British Columbia V6T 1Z3, Canada

Supporting Information

ABSTRACT: A structurally and compositionally well-defined and spectrally tunable artificial light-harvesting system has been constructed in which multiple organic dyes attached to a three-arm-DNA nanostructure serve as an antenna conjugated to a photosynthetic reaction center isolated from *Rhodobacter sphaeroides* 2.4.1. The light energy absorbed by the dye molecules is transferred to the reaction center, where charge separation takes place. The average number of DNA three-arm junctions per reaction center was tuned from 0.75 to 2.35. This DNA-templated multichromophore system serves as a modular light-harvesting antenna that is capable of being optimized for its spectral properties, energy transfer efficiency, and photostability, allowing one to adjust both the size and spectrum of the resulting structures. This may serve as a useful test bed for developing nanostructured photonic systems.

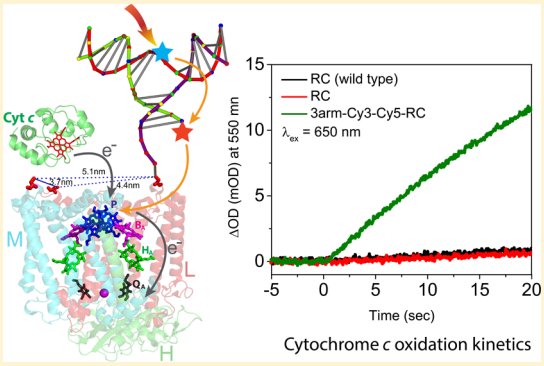

INTRODUCTION

During photosynthesis, light energy is collected by a large light-harvesting network and efficiently transferred to a reaction center (RC), which converts it to chemical energy via charge separation.[1] The quantum efficiency of the charge separation reaction by the photosynthetic reaction center is nearly unity.[1d] The architecture and spectral properties of the light-harvesting system that surrounds the reaction center have evolved to meet the constraints of a broad range of different light conditions and environments. A number of researchers have attempted to mimic the natural photosynthetic apparatus by designing artificial light-harvesting antenna systems[2−5] for a variety of photonic applications.[6]

To facilitate nanoscale photonic applications more broadly, the construction of artificial antenna systems that provide controllable light absorption, efficient energy transfer, and improved photostability is desirable. Self-assembling proteins[3] and dendrimers[4] have been explored to create artificial antenna systems, but they lack a well-defined multichromophore geometry and stoichiometry. Synthetic porphyrin structures[5] have been investigated to create artificial antennas connected to electron transfer complexes, but these generally have an absorption cross-section that is spectrally relatively narrow. DNA nanotechnology can be used to generate programmable, self-assembled nanostructures[7] with multiple fluorophores at well-defined positions, and this approach has been used to create artificial light-harvesting antenna systems. Double-helical DNA structures, three-way junctions, seven-helix bundles, and several other DNA-based antenna systems[8] have been used to create artificial antennas with unidirectional energy transfer along an excited-state energy gradient between chromophores that mimic the stepwise energy transfer in some of the natural photosynthetic systems. However, thus far these assemblies have lacked the ability to convert the light energy to redox energy via charge separation.

Recently, we have studied different dye molecules directly conjugated to reaction centers and explored the effects of altering the dye spectral and excited-state properties on the efficiency of energy transfer and charge separation.[9] In this report, we go a step further and use a three-arm-DNA nanostructure to organize multiple dye molecules and specifically assemble these nanostructured complexes with reaction centers (Figure 1A), resulting in a geometrically programmable model system mimicking a natural photosynthetic apparatus.

Two different pairs of DNA-conjugated chromophores are used in this study: Cy3 and Cy5, or Alexa Fluor 660 and Alexa Fluor 750. Cy3 acts as the donor and Cy5 as the acceptor in the first pair, and AF660 acts as the donor and AF750 as the acceptor in the second pair. The fluorophores were chosen such that there is significant spectral overlap between emission of the dyes and the absorption of the RC to facilitate efficient energy transfer, so that there is a substantial increase in the absorption cross-section in the spectral regions where the absorbance of the RC alone is low (Figures 1B, C and 3). A very simple three-

Received: September 2, 2014

   dx.doi.org/10.1021/ja509018g | J. Am. Chem. Soc. XXXX, XXX, XXX−XXX

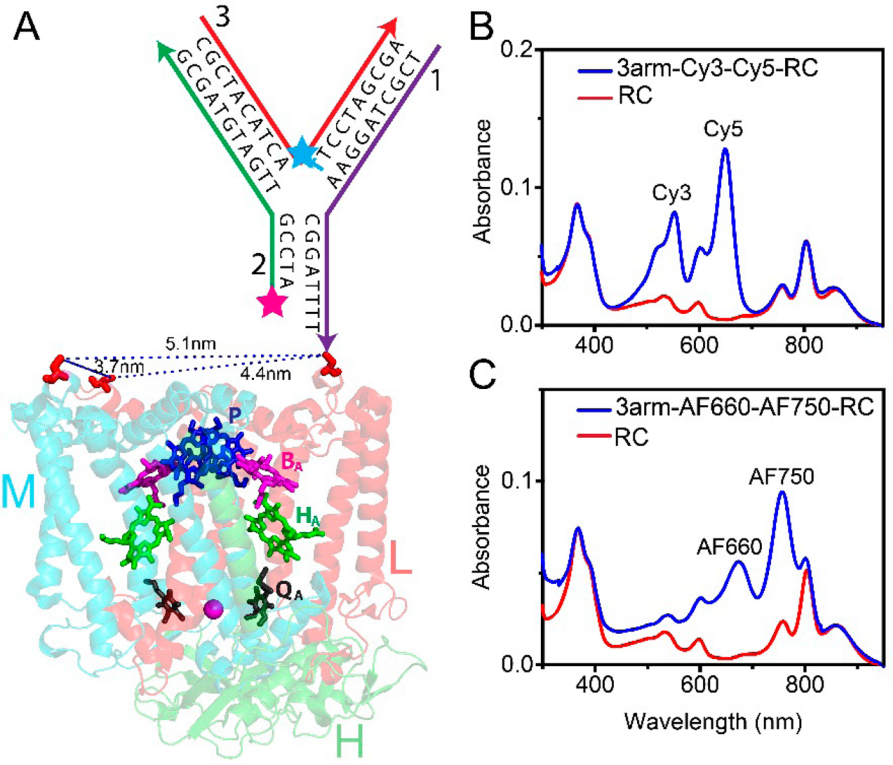

Figure 1. (A) Modified structure of the reaction center (RC) from the purple bacterium *Rhodobacter sphaeroides* 2.4.1 (PDB 2J8C[10]) with sequences of the three-arm-DNA construct shown. The cofactors of the RC are colored and those active in electron transfer reactions involved in this report are designated by letters: P, bacteriochlorophyll pair; B_A, bacteriochlorophyll monomer; H_A, bacteriopheophytin; Q_A, ubiquinone. The arrows in the DNA structure point in direction of the 3′-end of the DNA strands. The 3′-amine-modified strand-1 (purple) of the three-arm DNA is conjugated to one of the Cys residues (shown in red) on the surface of the RC via an *N*-succinimidyl 3-(2-pyridyldithio)propionate linker. The other two strands (strand-2 and -3, in green and red, respectively) are allowed to hybridize to strand-1 to form the three-arm-DNA junction. Inter-Cys distances on the RC are marked as dotted lines. The two stars on the three arms represent the positions of the two dye molecules, where the cyan star corresponds to either Cy3 or AF660 and the pink star corresponds to either Cy5 or AF750. It should be noted that because of the presence of three Cys residues on the surface of the protein, one, two, or three copies of strand-1 can be conjugated to the RC, and consequently, up to three three-arm-DNA junctions (and three pairs of dyes) can be conjugated to the RC. For clarity, only one is shown here. (B) A representative absorption spectrum of RCs that have an average of 2.3 of the 3-arm-DNA−Cy3-Cy5 nanostructures attached. (C) An absorbance spectrum of RCs that have an average of 2.1 of the 3-arm-DNA−AF660-AF750 nanostructures attached. The absorbance spectra of panels B and C show enhanced absorbance cross-section in the spectral regions 450−700 or 500−800 nm, respectively, where the RC absorbance is relatively low. The spectrum of free RC is shown in both panels B and C (red trace) for comparison.

arm-DNA structure was designed to assemble the two dye molecules in a geometrically defined manner and to avoid chemical modification of any DNA strands with more than one dye (to reduce cost and synthetic complexity) (Figure 1A). Two of the strands (strand-2 and -3) in the three-arm DNA contain the dye molecules, and the other one (strand-1) is conjugated to the RC through a covalent cross-link.

The three-dimensional structure of the RC complex from *R. sphaeroides* 2.4.1[10] is depicted in Figure 1A, and it consists of three subunits, H, M, and L. There is a total of 10 cofactors associated with the L/M transmembrane region of the structure, including a dimer of bacteriochlorophylls (P), two monomer bacteriochlorophylls (B_A and B_B), two bacteriopheophytins (H_A and H_B), two ubiquinone-10 molecules (Q_A and Q_B), one carotenoid, and one non-heme iron (Fe^{2+}).[11] The special pair P is the primary donor of electrons in the light-driven electron transfer process, which subsequently transfers electron to Q_A via B_A and H_A, forming a long-lived charge-separated state $P^+Q_A^-$. When ubiquinone is bound in the Q_B site, electron transfer occurs from Q_A^- to Q_B, forming $P^+Q_B^-$.[12]

A genetically modified RC was used in these studies and contained a total of eight mutations, five of them to replace the five wild-type cysteines with serine or alanine and the remaining three to replace three selected wild-type amino acids (asparagine or glutamic acid) with cysteine residues at specific locations on the surface of the RC that are close to the primary electron donor, P.[9b,13] Two of the new Cys residues are located on the surface of the L subunit (L72, L274) and the other one is on the surface of the M subunit (M100) (Figure 1A).

RESULTS AND DISCUSSION

Assembly of Light-Harvesting/Reaction Center Complex. The 3′-amine-modified strand-1 was conjugated to the introduced Cys residues of the RC in a 10:1 molar ratio by using an SPDP [*N*-succinimidyl 3-(2-pyridyldithio)propionate] cross-linker (see details in the Supporting Information). The reaction mixture was subsequently purified by fast protein liquid chromatography (FPLC) (Figure 2) (see the Supporting Information for methods). The chromatograph shows four prominent peaks using absorbance at 260 and 280 nm and three peaks using absorbance at 365 nm (Soret peak of RC). The fractions under each peak were collected and characterized. The UV−vis absorbance maxima for the first, second, and third peaks in the chromatograph are at 271, 268, and 266 nm,

dx.doi.org/10.1021/ja509018g | J. Am. Chem. Soc. XXXX, XXX, XXX−XXX

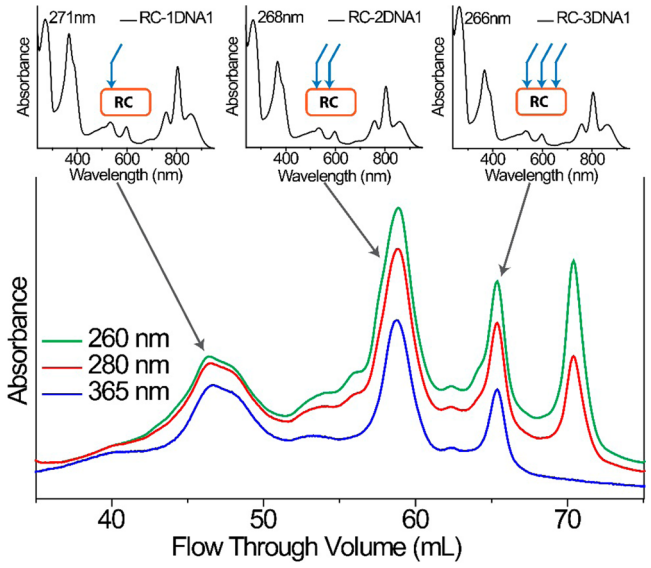

Figure 2. FPLC purification trace of DNA-conjugated (strand-1) RCs. Chromatographs at 260 nm (green), 280 nm (red), and 365 nm (blue) are shown. The absorbance bands at 260 and 280 nm are from both RC and DNA, whereas the absorbance bands at 365 nm are from the RC. The fractions from each of the peaks were collected separately and their respective absorbance spectra measured. Representative absorbance spectra showing the number of DNA strands conjugated per RC are given at the top of the figure.

respectively. The blue shift of the absorbance peak, together with a relative increase in the absorbance intensity (compared to the absorbance peak at 800 nm), indicates that the species contained in the peaks have different ratios of DNA conjugated to the RC, increasing from peak 1 to peak 3. (DNA:RC = 1:1, 2:1, and 3:1).

It is important to note that the single copy of strand-1 conjugated to RC can be on any of the three Cys. Similarly, there are three ways that two copies of strand-1 could be conjugated to the RC. This heterogeneity of the sample is reflected by the widths of the first and second chromatograph peaks. The third peak, in contrast, has the narrowest peak and highest ratio of A260/A365 among the first three, and it represents a single species of RC with three copies of strand-1 conjugated to all of the Cys residues. The last peak in the chromatograph has no absorbance at 365 nm (the Soret absorbance band of the RC), indicating that it is excess free ssDNA with no RC attached.

Dye-labeled, preannealed strand-2 and -3 are then allowed to hybridize to the purified strand-1-conjugated RC to create 3-arm-DNA–RC conjugates with one, two, or three three-arm-DNA junctions on each RC (Schemes S3 and S4, Supporting Information) carrying different identities and numbers of dyes. Cy3-modified strand-3 and Cy5-modified strand-2 were purchased from Integrated DNA Technologies (IDTDNA). AF660-modified strand-3 and AF750-modified strand-2 were synthesized by reacting amine-modified DNA (strand-2 or -3, synthesized using a DNA synthesizer) with the succinimidyl ester of the corresponding dye (purchased from Invitrogen). The resulting conjugate was subsequently purified by reverse-phase HPLC and characterized using matrix-assisted laser desorption ionization time-of-flight (MALDI-TOF) mass spectroscopy (see details in the Supporting Information, Figure S1).

The assembly of the 3-arm-DNA–RC constructs containing only Cy3 and different DNA/RC ratios are named **1C**, **2C**, or **3C** (abbreviations as in Table 1). These were created by assembling strand-2 (unmodified) and Cy3-modified strand-3 with the FPLC fractions that contained conjugates of one, two, or three Strand-1 conjugates per RC. The spectra of these structures show enhanced absorbance between 450 and 580 nm compared to the RC alone, due to the additional absorbance from Cy3 in this spectral region [Figures 3A and S5 (Supporting Information)]. Three-arm-DNA nanostructure to RC ratios of 0.75 ± 0.05, 1.65 ± 0.05, and 2.35 ± 0.05 were

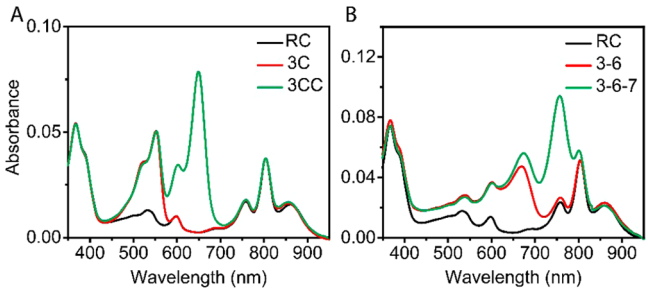

Figure 3. Absorption spectra of representative 3-arm-DNA–dye–RC constructs. (A) Absorption spectra of RC, **3C**, and **3CC**. (B) Absorption spectra of RC, **3–6**, and **3–6–7**.

Table 1. Three-Arm DNA to RC Ratio of Different Constructs

dye	sample	abbreviation	3-arm/RC[a]
Cy3/Cy5	3-arm–Cy3–RC(1DNA)	**1C**	0.75 ± 0.05
	3-arm–Cy3–RC(2DNA)	**2C**	1.65 ± 0.05
	3-arm–Cy3–RC(3DNA)	**3C**	2.35 ± 0.05
	3-arm–Cy3-Cy5–RC(1DNA)	**1CC**	0.8 ± 0
	3-arm–Cy3-Cy5–RC(2DNA)	**2CC**	1.65 ± 0.05
	3-arm–Cy3-Cy5–RC(3DNA)	**3CC**	2.2 ± 0.1
AF660/AF750	3-arm–660–RC(1DNA)	**1–6**	0.85 ± 0.15
	3-arm–660–RC(2DNA)	**2–6**	1.6 ± 0
	3-arm–660–RC(3DNA)	**3–6**	2.15 ± 0.05
	3-arm–660-750–RC(1DNA)	**1–6–7**	0.9 ± 0.1
	3-arm–660-750–RC(2DNA)	**2–6–7**	1.65 ± 0.05
	3-arm–660-750–RC(3DNA)	**3–6–7**	2.0 ± 0.1

[a]The molar ratios of the 3-arm/RC were obtained by measuring the dye concentration and the RC concentration, calculated from their UV–vis absorbance spectra and known absorption coefficients, assuming that the HPLC-purified DNA strands were fully labeled with their respective dyes.

dx.doi.org/10.1021/ja509018g | J. Am. Chem. Soc. XXXX, XXX, XXX–XXX

calculated on the basis of the UV−vis absorbance spectra for **1C**, **2C**, and **3C** (see the footnote of Table 1). Apparently, the yield of assembly for the fully loaded three-arm-DNA junction on the RC was ∼75−80%. This <100% yield may be due to local steric effects near the protein surface that reduce the DNA hybridization yield. The similarly assembled 3-arm-DNA−RC constructs containing one, two, and three copies of both Cy3- and Cy5-labeled DNA strands are named **1CC**, **2CC**, and **3CC** (Table 1), and the spectral analysis revealed that they have three-arm-DNA nanostructure to RC ratios of 0.8 ± 0, 1.65 ± 0.05, and 2.2 ± 0.1, respectively [Figures 3A and S6 (Supporting Information)]. Apparently adding the second dye molecules (covalently modified on the 5′-end of strand-2) did not affect the DNA hybridization yield. When both Cy3 and Cy5 are present (as in **1CC**, **2CC**, and **3CC**), they absorb significantly between 450 and 700 nm. Similarly, the 3-arm-DNA−RC constructs containing different numbers of AF660 only (abbreviated as **1−6**, **2−6**, and **3−6**) and different numbers of both AF660 and AF750 (abbreviated as **1−6−7**, **2−6−7**, and **3−6−7**) provide strong absorbance between 500 and 800 nm [Figures 3B and S7 and S8 (Supporting Information)]. The three-arm DNA to RC ratios for the different constructs are listed in Table 1.

Excitation Energy Transfer Efficiency. The efficiency and kinetics of the FRET (Förster resonance energy transfer) process for each construct was investigated using steady-state and time-resolved fluorescence spectroscopy (see Supporting Information for calculations). The free three-arm-DNA constructs with respective dye(s) attached (without the RC) were used as control samples for these experiments (Figures S3 and S4, Supporting Information). Upon exciting **3C** at 510 nm, 30% of the Cy3 emission was quenched compared to that of 3-arm-DNA−Cy3, presumably due to energy transfer from Cy3 to the RC [Figures 4A and S5C (Supporting Information)]. In

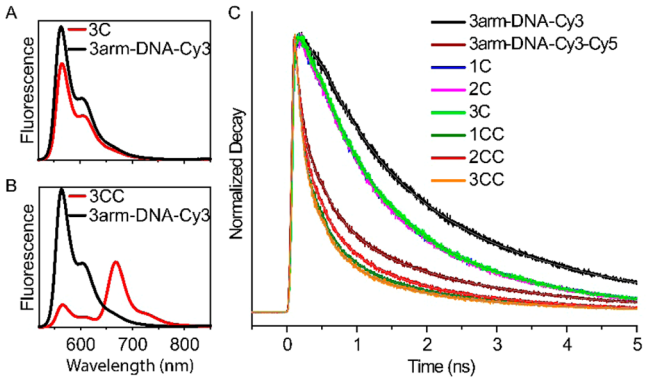

Figure 4. Fluorescence emission spectra of **3C** (A) and **3CC** (B) in comparison with emission spectra of 3-arm-DNA−Cy3 (λ_{ex} = 510 nm). (C) Cy3 fluorescence decay profiles of free three-arm DNA and three-arm DNA conjugated to the RC in various ratios, with either constructs containing Cy3 alone (**1C**, **2C**, **3C**) or constructs with both Cy3 and Cy5 (**1CC**, **2CC**, **3CC**), monitored at 565 nm (λ_{ex} = 510 nm).

the case of **3CC**, there was an 84% decrease in Cy3 emission intensity compared to that of 3-arm-DNA−Cy3 without the RC [Figures 4B and S6 (Supporting Information)]. Comparing **3C** and **3CC**, the greater decrease in fluorescence of Cy3 when Cy5 was present is attributed to the summation of multiple energy transfer pathways; a direct energy transfer from Cy3 to the RC and a stepwise energy transfer from Cy3 to Cy5 to the RC. Compared with the 3-arm-DNA−Cy3-Cy5 alone with no RC, **3CC** (with both dyes in the same three-arm DNA that is linked to the RC) shows a 45% decrease in total fluorescence intensity integrated from 520 to 850 nm upon Cy3 excitation (Figure S6, Supporting Information). On the other hand, upon Cy5 excitation at 620 nm, the direct FRET efficiency of Cy5 to the RC in **3CC** is calculated to be 48%, using the emission of the 3-arm-DNA−Cy3-Cy5 as a reference (Figure S6, Supporting Information).

Similar experiments were performed on all the other 3-arm-DNA−dye−RC constructs, and the energy transfer efficiency values obtained are shown in Figures 5, S5−S8, and S11 (Supporting Information). Samples with different ratios of 3-arm-DNA−dye conjugate to RC (for example, compare **1C**, **2C**, and **3C**, or **1−6**, **2−6**, and **3−6**) all yielded similar energy transfer efficiency values between the individual dyes and the RC or between the dyes together and the RC. This is due to the fact that although there are multiple dye molecules on the assembled structures, the probability of exciting more than one dye molecule associated with a particular RC at any time is very low due to the continuous nature and low intensity of the excitation light. Moreover, as expected, the efficiency of energy transfer from AF650 to the RC (∼55%) is higher than the efficiency of Cy3 transfer to the RC (∼35%) [comparing Figure 5 and S11 (Supporting Information)]. This is presumably due to the greater spectral overlap between the emission of AF660 and the absorbance of the RC compared to that of Cy3. However, even though AF750 has a greater spectral overlap with RC than does Cy5, it has a lower energy transfer efficiency to RC (∼42%) than Cy5 does (∼52%), and this results in a higher overall energy transfer efficiency of the Cy3−Cy5 pair to the RC (∼83%) than the AF660−AF750 pair (∼75%). We have observed similar phenomena earlier,[9b] and the reason for the lower energy transfer efficiency of AF750 to RC is the shorter intrinsic lifetime of AF750 compared to that of Cy5.

Time-resolved fluorescence analysis was performed using time-correlated single-photon counting (TCSPC) [Figures 4C and S9 and S10 (Supporting Information)] excited by a pulsed laser. The decay traces of individual-dye-labeled three-arm DNA (only one dye on the three-arm DNA without the RC) could be fitted adequately with biexponential decay kinetics[8a,9b] [Tables 2 and S1−S3 (Supporting Information)]. The amplitude-weighted average lifetimes were 1.79 ns for Cy3, 1.65 ns for Cy5, 1.68 ns for AF660, and 0.64 ns for AF750. In contrast, fitting the fluorescence decays for each of the 3-arm-DNA−dye−RC constructs required three or four exponential components [Tables 2 and S1−S3 (Supporting Information)]. For example, considering the decay profiles of Cy3 in various samples (λ_{ex} = 510 nm and λ_{em} = 565 nm in Figure 4), a substantial increase in the fluorescence decay rate is observed for the constructs with the RC; e.g., the average lifetimes of **3C** and **3CC** are ∼1.17 and ∼0.25 ns, respectively. This follows the same trend as the steady-state energy transfer measurements and again implies that a significant amount of energy transfer takes place from the dye to the RC. Similar decay patterns were observed for the set of constructs with Alexa Fluor dyes (Figure S10, Supporting Information). On the basis of the lifetime data for the dyes alone (without RCs) or one dye with the RC, the rate constants for various component processes can be determined as described in the Supporting Information. For example, the fluorescence decay rate constant for Cy3 alone (in the absence of Cy5 or RC) is measured to be 0.55 ns^{-1}, the rate constant for energy transfer from Cy3 to the RC is calculated to

dx.doi.org/10.1021/ja509018g | J. Am. Chem. Soc. XXXX, XXX, XXX−XXX

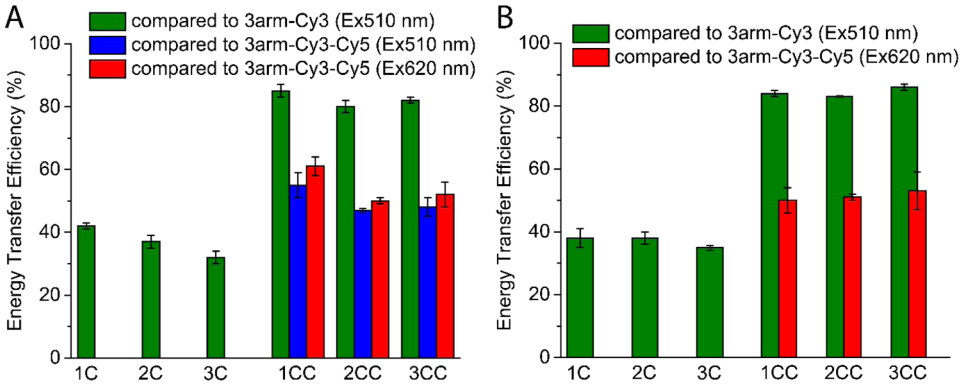

Figure 5. Energy transfer efficiency of three-arm-DNA-conjugated RC calculated from (A) steady-state data and (B) from lifetime data. The green bars show the energy transfer efficiency calculated by comparing fluorescence from the RC-containing complex with that from the three-arm DNA containing only Cy3 (without RC). The blue and red bars are the energy transfer efficiency values calculated with excitation of Cy3 and Cy5, respectively, using the three-arm DNA containing both the dyes (Cy3-Cy5) without the RC attached as the fluorescence reference. The FRET efficiencies (E) from steady-state fluorescence data were calculated according to the following equation: $E = 1 - [(I_{DA}/A_{DA})/(I_D/A_D)]$, where I_{DA} and I_D are the integrated area of fluorescence from the donor with and without an acceptor. A_{DA} and A_D are the absorbance of the donor at excitation wavelength with and without an acceptor. The energy transfer efficiencies ($E_{lifetime}$) from lifetime data were calculated according to the following equation: $E_{lifetime} = 1 - (\tau_{ave,DA}/\tau_{ave,D})$, where $\tau_{ave,DA}$ and $\tau_{ave,D}$ are the average lifetime of the donor (Table 2) with and without an acceptor.

Table 2. Fitting Parameters for the Cy3 Lifetime Data in Different Constructs, Monitored at 565 nm (λ_{ex} = 510 nm)[a]

sample	τ_1, ns (amplitude %)	τ_2, ns (amplitude %)	τ_3, ns (amplitude %)	τ_4, ns (amplitude %)	κ^2	average lifetime (ns)[b]
3-arm-DNA−Cy3	0.63 (34.9)	2.41 (65.1)	–	–	1.18	1.788
	0.64 (35.5)	2.45 (64.5)	–	–	1.17	1.807
3-arm-DNA−Cy3-Cy5	0.06 (59.8)	0.40 (22.9)	2.15 (17.3)	–	1.17	0.499
	0.07 (52.7)	0.52 (23.6)	2.19 (23.7)	–	1.16	0.678
1C	0.12 (14.1)	0.68 (45.0)	1.80 (40 9)	–	1.03	1.059
	0.09 (12.1)	0.67 (42.7)	1.90 (45.2)	–	1.01	1.156
2C	0.12 (12.8)	0.71 (43.3)	1.89 (43.9)	–	1.06	1.152
	0.09 (11.5)	0.66 (46.5)	1.80 (42.0)	–	1.07	1.073
3C	0.10 (12.5)	0.70 (42.3)	1.90 (45.2)	–	1.05	1.167
	0.11 (13.2)	0.75 (45.4)	1.96 (41.4)	–	1.14	1.167
1CC	0.04 (50.9)	0.15 (28.7)	0.59 (11.5)	1.86 (8.9)	1.05	0.297
	0.03 (51.5)	0.15 (29.1)	0.54 (11.1)	1.85 (8.3)	1.04	0.272
2CC	0.04 (49.0)	0.14 (28.1)	0.53 (12.7)	1.81 (10.2)	1.00	0.311
	0.03 (47.0)	0.14 (29.8)	0.56 (12.9)	1.85 (10.3)	1.07	0.318
3CC	0.04 (51.4)	0.14 (29.2)	0.51 (11.4)	1.79 (8.0)	1.07	0.263
	0.03 (53.6)	0.14 (27.3)	0.48 (11.7)	1.75 (7.4)	1.02	0.240

[a]The results from two replicates of each sample are shown. [b]Average lifetime is calculated as $\tau_{ave} = \sum_i A_i\tau_i/\sum_i A_i$, where A_i is the amplitude of the ith component and τ_i is the corresponding lifetime.

be 0.39 ns^{-1}, and the rate constant for energy transfer from Cy3 to Cy5 is calculated to be 1.45 ns^{-1}. If one uses the rate constants for these individual processes to calculate the decay lifetime of Cy3 in the fully assembled complex (**1CC**), it is predicted to be 0.42 ns, whereas the experimentally measured average lifetime is 0.28 ns. Similarly, the experimentally observed lifetime of AF660 is 0.90 ns in **1**−**6**−**7**, and the predicted decay lifetime of AF660 in **1**−**6**−**7** is 0.92 ns (on the basis of the measurements of the decay lifetime of AF660 alone, the energy transfer rate constants from AF660 to AF750 and from AF660 to RC). The approximate agreement of the experimentally measured decay times for the full nanostructures and the predicted values based on the kinetic constants for individual component reactions indicates that the experimental measurements are internally consistent with each other and consistent with an overall picture of stepwise energy transfer.

Further evidence of a stepwise energy transfer process is provided by the initial rise of the Cy5 and AF750 emission in the TCSPC experiment in the two dye complexes, upon excitation of Cy3 and AF660, respectively (Figures S9 and S10, Supporting Information). The Cy3 or AF670 in all cases shows an instantaneous increase of the emission upon direct excitation (which is convoluted with the instrument response function); the rise of the Cy5 or AF750s emission without RC is much slower than the instrument response. This is due to the energy transfer from the initial donor (Cy3 or AF660) to the intermediate dye (Cy5 or AF750) on the subnanosecond time scale, which results in an initial increase in the excited-state population of the intermediate. In the presence of the RC, Cy5 or AF750 shows a much faster decay. A comparison of the average lifetimes of the dyes in the 3-arm-DNA−RC constructs vs. that in the three-arm-DNA structures (without RC) results in estimated energy-transfer efficiencies from the dyes to the RC [Figures 5B and S11B (Supporting Information)] that are in reasonable agreement with the results obtained from the steady-state fluorescence intensity measurements [Figures 5A and S11A (Supporting Information)]. Like the steady-state measurements, similar energy-transfer efficiencies are observed

dx.doi.org/10.1021/ja509018g | J. Am. Chem. Soc. XXXX, XXX, XXX−XXX

for samples with different numbers of DNA−dye constructs per RC. Again, in the case of time-resolved measurements, higher energy-transfer efficiency is observed for constructs that contain Cy5 compared to AF750, even though the fluorescence spectrum of AF750 overlaps better with the absorbance of the RC than does that of Cy5. This can be explained by the fact that AF750 has a shorter excited-state lifetime (0.64 ns) than Cy5 (1.64 ns), which gives the excited state of Cy5 a greater probability of transferring energy to the RC before decaying to the ground state by other pathways. Similar results were obtained previously when dye molecules with different lifetimes were conjugated directly to the RC.[9b]

Enhancement of Reaction Center Charge Separation. Because charge separation in the RC has an almost unity yield, the amount of charge separation that takes place correlates with the energy transfer efficiency.[9b] The relative amount of charge separation in the RC was investigated by measuring the light-minus-dark difference absorbance spectra of the different dye−DNA−RC complexes. The difference spectra were obtained by subtracting the absorbance spectrum of a sample taken in the dark from the absorbance spectrum taken under continuous illumination at 550 nm (Cy3 absorbance peak, 10 nm bandwidth). The light intensity at 550 nm was kept low enough to ensure that the light-minus-dark signals changed linearly with the light energy absorbed. Under low-light conditions, no RC is excited more than once during the ~100 ms lifetime of $P^+Q_A^-$, avoiding artifacts due to photopumping. A 1.3-fold larger absorbance change at 862 nm (reflecting P^+ formation) was observed for **3C** compared to the RC alone, implying enhanced charge-separated state formation due to the increased absorbance cross section at 550 nm, confirming that photons absorbed by Cy3 result in energy transfer to RC cofactors (Figure 6). Similarly, **3CC**

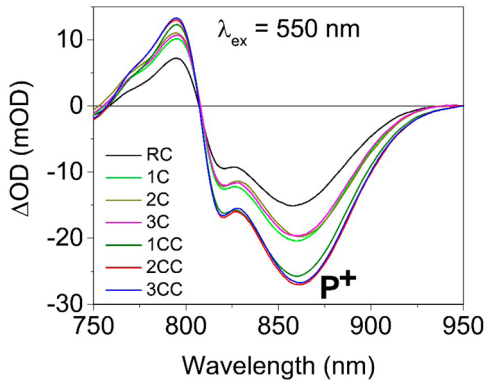

Figure 6. Light-minus-dark difference absorbance spectra of RCs with and without conjugation to a 3-arm-DNA−dye complex.

shows a 1.8-fold enhancement in P^+ formation over unconjugated RCs. The enhanced P^+ formation in **3CC** compared to **3C** presumably results from the higher efficiency of the overall stepwise energy transfer from Cy3 to Cy5 to the RC, compared to direct transfer from Cy3 to the RC (Figure 5). The insertion of Cy5 between Cy3 and the RC results in two relatively efficient transfer steps (better spectral overlap and shorter distance) compared to the single Cy3 to RC transfer. As with the energy transfer efficiency results obtained from both the steady-state and the time-resolved fluorescence measurements, the relative intensity of P^+ formation is similar for samples with different numbers of three-arm-DNA nanostructures conjugated to each RC (i.e., similarity among the samples **1C**, **2C** and **3C** or among the samples **1CC**, **2CC** and **3CC**).

In the purple bacteria, the RC operates in conjunction with the cytochrome bc_1 complex, cytochrome c_2, and a quinone pool, to convert light energy into a proton motive force.[14] In this process, the oxidized initial electron donor of the RC, P^+, that is formed upon light-driven electron transfer is subsequently reduced by cytochrome c_2, which docks to the periplasmic face (P side) of the RC. In our artificial antenna system, the three-arm-DNA structures are located on the P side of RC, and so one might expect that this conjugation of DNA close to the docking site of cytochrome would hinder cytochrome binding as well as the electron transfer process from cytochrome to P^+. To explore this possibility, a 10-fold molar excess of reduced cytochrome c[15] and a 100-fold molar excess of decylubiquinone were added into a solution of 3-arm-DNA−dye−RC constructs, and the absorbance intensity change at 550 nm (an absorbance decrease at this wavelength reflects the oxidation of cytochrome c) was measured, while either exciting the RC directly or the dye directly.[9,16] Using 800 nm excitation (direct excitation of the RC), where both the Cy3 and Cy5 have no absorbance, the wild-type RC, the Cys-modified RC, and the RC conjugated with the DNA−dye construct all showed similar rates of cytochrome c oxidation (Figure 7A). Apparently, DNA conjugation does not hinder the rate of cytochrome electron transfer to the RC, at least at these concentrations. However, upon 650 nm excitation (Cy5 excitation peak), the DNA−dye-conjugated RC showed a much faster rate of oxidation then did the Cys-modified RC or wild-type RC, both of which have very low absorbance at 650 nm (Figure 7B). It is interesting to note that under the conditions of this kinetic measurement, the oxidation rate of cytochrome c depends on the number of dye molecules in the construct. This presumably results from the enhanced absorbance cross-section of the light-harvesting antenna that increases the number of photons absorbed per unit time by the 3-arm-DNA−dye−RC complex. The cytochrome c oxidation experiment is real-time and reports the cumulative result (i.e., integration of the change over time). Since the spectrum of reduced cytochrome c overlaps strongly with that of Cy3, making it difficult to quantify the number of photons absorbed by Cy3, similar measurements using 550 nm excitation were not attempted.

■ CONCLUSIONS

A DNA nanostructure with dyes attached at specific positions was conjugated to a RC to serve as a geometrically defined light-harvesting antenna. This extended the absorbance cross section of the complex into a spectral range where the RC has only weak absorbance. A combination of factors, including the spatial placement, spectral properties, and excited state kinetic properties of the dyes used, is important in determining the efficiency of the antenna in energy transfer. At low-light flux, the rate of photon capture by the complex is proportional to the number of dye molecules in the complex that absorb at the excitation wavelength; thus, increasing the number of DNA−dye constructs attached to the reaction center increases the functional cross section but does not greatly change the energy transfer efficiency. The complexes explored in this work provide useful model systems for future applications in nanophotonics.

dx.doi.org/10.1021/ja509018g | J. Am. Chem. Soc. XXXX, XXX, XXX−XXX

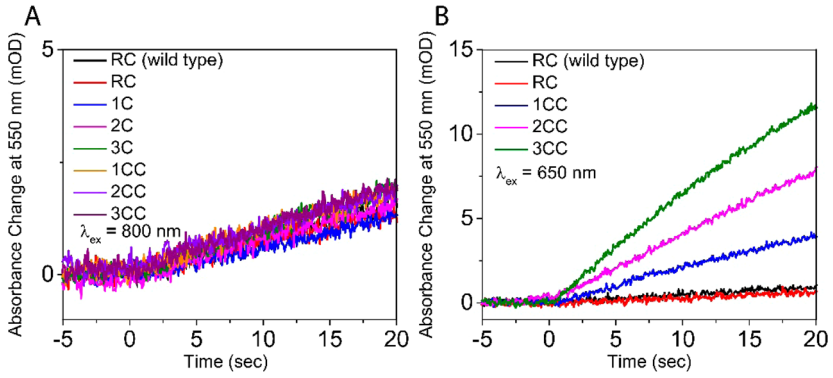

Figure 7. Cytochrome *c* oxidation monitored at 550 nm (where the difference in absorbance between reduced and oxidized cytochrome *c* is maximal) after exciting the RC directly at 800 nm (A) or Cy5 directly at 650 nm (B).

■ ASSOCIATED CONTENT

Supporting Information

Methods, calculations, gel electrophoresis, DNA sequences, additional spectral data, and DNA synthesis and modification characterization. This material is available free of charge via the Internet at http://pubs.acs.org.

■ AUTHOR INFORMATION

Corresponding Authors

nwoodbury@asu.edu
Hao.Yan@asu.edu

Notes

The authors declare no competing financial interest.

■ ACKNOWLEDGMENTS

We thank Douglas Daniel for his help in setting up the spectroscopy for the light-minus-dark experiment. This research was supported by Multidisciplinary University Research Initiative (MURI) program (award W911NF-12-1-0420) funded by Army Research office (ARO) to H.Y. and N.W.W. and a grant from the Canadian Natural Sciences and Engineering Research Council to J.T.B.

■ REFERENCES

(1) (a) Blankenship, R. E. *Molecular Mechanisms of Photosynthesis*; Blackwell Science: Oxford, U.K., 2002. (b) Scholes, G. D.; Fleming, G. R.; Olaya-Castro, A.; van Grondelle, R. *Nat. Chem.* **2011**, *3*, 763. (c) McDermott, G.; Prince, S. M.; Freer, A. A.; Hawthornthwaite-Lawless, A. M.; Papiz, M. Z.; Cogdell, R. J.; Isaacs, N. W. *Nature* **1995**, *374*, 517. (d) Wraight, C. A.; Clayton, R. K. *Biochim. Biophys. Acta* **1974**, *333*, 246.

(2) (a) Schenning, A. P. H. J.; Benneker, F. B. G.; Geurts, H. P. M.; Liu, X. Y.; Nolte, R. J. M. *J. Am. Chem. Soc.* **1996**, *118*, 8549. (b) Jullien, L.; Canceill, J.; Valeur, B.; Bardez, E.; Lefèvre, J.-P.; Lehn, J.-M.; Marchi-Artzner, V.; Pansu, R. *J. Am. Chem. Soc.* **1996**, *118*, 5432. (c) Würthner, F.; Sautter, A. *Org. Biomol. Chem.* **2003**, *1*, 240. (d) Choi, M.-S.; Yamazaki, T.; Yamazaki, I.; Aida, T. *Angew. Chem., Int. Ed.* **2004**, *43*, 150. (e) Sautter, A.; Kaletaş, K. K.; Schmid, D. G.; Dobrawa, R.; Zimine, M.; Jung, G.; Stokkum, I. H. M.; De Cola, L.; Williams, R. M.; Würthner, F. *J. Am. Chem. Soc.* **2005**, *127*, 6719. (f) Nakamura, Y.; Aratani, N.; Osuka, A. *Chem. Soc. Rev.* **2007**, *36*, 831. (g) Terazono, Y.; Kodis, G.; Liddell, P. A.; Garg, V.; Moore, T. A.; Moore, A. L.; Gust, D. *J. Phys. Chem. B* **2009**, *113*, 7147. (h) Boeneman, K.; Deschamps, J. R.; Buckhout-White, S.; Prasuhn, D. E.; Blanco-Canosa, J. B.; Dawson, P. E.; Stewart, M. H.; Susumu, K.; Goldman, E. R.; Ancona, M.; Medintz, I. L. *ACS Nano* **2010**, *4*, 7253. (i) Boeneman, K.; Prasuhn, D. E.; Blanco-Canosa, J. B.; Dawson, P. E.; Melinger, J. S.; Ancona, M.; Stewart, M. H.; Susumu, K.; Huston, A.; Medintz, I. L. *J. Am. Chem. Soc.* **2010**, *132*, 18177. (j) Hannestad, J. K.; Sandin, P.; Albinsson, B. *J. Am. Chem. Soc.* **2008**, *130*, 15889.

(3) (a) Miller, R. A.; Presley, A. D.; Francis, M. B. *J. Am. Chem. Soc.* **2007**, *129*, 3104. (b) Ma, Y.-Z.; Miller, R. A.; Fleming, G. R.; Francis, M. B. *J. Phys. Chem. B* **2008**, *112*, 6887. (c) Miller, R. A.; Stephanopoulos, N.; McFarland, J. M.; Rosko, A. S.; Geissler, P. L.; Francis, M. B. *J. Am. Chem. Soc.* **2010**, *132*, 6068. (d) Endo, M.; Fujitsuka, M.; Majima, T. *Chem.—Eur. J.* **2007**, *13*, 8660. (e) Scolaro, L. M.; Castriciano, M. A.; Romeo, A.; Micali, N.; Angelini, N.; Lo Passo, C.; Felici, F. *J. Am. Chem. Soc.* **2006**, *128*, 7446. (f) Nam, Y. S.; Shin, T.; Park, H.; Magyar, A. P.; Choi, K.; Fantner, G.; Nelson, K. A.; Belcher, A. M. *J. Am. Chem. Soc.* **2010**, *132*, 1462.

(4) (a) Schenning, A. P. H. J.; Peeters, E.; Meijer, E. W. *J. Am. Chem. Soc.* **2000**, *122*, 4489. (b) Adronov, A.; Fréchet, J. M. J. *Chem. Commun.* **2000**, 1701. (c) Weil, T.; Reuther, E.; Müllen, K. *Angew. Chem., Int. Ed.* **2002**, *41*, 1900. (d) Choi, M.-S.; Aida, T.; Yamazaki, T.; Yamazaki, I. *Chem.—Eur. J.* **2002**, *8*, 2667. (e) Hahn, U.; Gorka, M.; Vögtle, F.; Vicinelli, V.; Ceroni, P.; Maestri, M.; Balzani, V. *Angew. Chem., Int. Ed.* **2002**, *41*, 3595. (f) Balzani, V.; Ceroni, P.; Maestri, M.; Vicinelli, V. *Curr. Opin. Chem. Biol.* **2003**, *7*, 657. (g) Imahori, H. *J. Phys. Chem. B* **2004**, *108*, 6130. (h) Cotlet, M.; Vosch, T.; Habuchi, S.; Weil, T.; Müllen, K.; Hofkens, J.; De Schryver, F. *J. Am. Chem. Soc.* **2005**, *127*, 9760.

(5) (a) Guldi, D. M. *Chem. Soc. Rev.* **2002**, *31*, 22. (b) Aratani, N.; Kim, D.; Osuka, A. *Acc. Chem. Res.* **2009**, *42*, 1922. (c) Guldi, D. M. *Pure Appl. Chem.* **2003**, *75*, 1069. (d) Harriman, A.; Sauvage, J.-P. *Chem. Soc. Rev.* **1996**, *25*, 41.

(6) Eisele, D. M.; Cone, C. W.; Bloemsma, E. A.; Vlaming, S. M.; van der Kwaak, C. G. F.; Silbey, R. J.; Bawendi, M. G.; Knoester, J.; Rabe, J. P.; Bout, D. A. V. *Nat. Chem.* **2012**, *4*, 655.

(7) (a) Seeman, N. C. *J. Theor. Biol.* **1982**, *99*, 237. (b) Seeman, N. C. *Mol. Biotechnol.* **2007**, *37*, 246. (c) Seeman, N. C. *Nano Lett.* **2010**, *10*, 1971. (d) Lin, C.; Liu, Y.; Rinker, S.; Yan, H. *ChemPhysChem* **2006**, *7*, 1641. (e) Aldaye, F. A.; Palmer, A. L.; Sleiman, H. F. *Science* **2008**, *321*, 1795. (f) Rothemund, P. W. K. *Nature* **2006**, *440*, 297. (g) Winfree, E.; Liu, F.; Wenzler, L. A.; Seeman, N. C. *Nature* **1998**, *394*, 539. (h) Sharma, J.; Chhabra, R.; Cheng, A.; Brownell, J.; Liu, Y.; Yan, H. *Science* **2009**, *323*, 112. (i) Hung, A. M.; Micheel, C. M.; Bozano, L. D.; Osterbur, L. W.; Wallraff, G. M.; Cha, J. N. *Nat. Nanotechnol.* **2010**, *5*, 121. (j) Zheng, J.; Constantinou, P. E.; Micheel, C.; Alivisatos, A. P.; Kiehl, R. A.; Seeman, N. C. *Nano Lett.* **2006**, *6*, 1502. (k) Sharma, J.; Ke, Y.; Lin, C.; Chhabra, R.; Wang, Q.; Nangreave, J.; Liu, Y.; Yan, H. *Angew. Chem., Int. Ed.* **2008**, *47*, 5157. (l) Deng, Z.; Samanta, A.; Nangreave, J.; Yan, H.; Liu, Y. *J. Am. Chem. Soc.* **2012**, *134*, 17424. (m) Maune, H. T.; Han, S.-p.; Barish, R. D.; Bockrath, M.; Goddard, W. A., III; Rothemund, P. W. K.; Winfree, E. *Nat. Nanotechnol.* **2010**, *5*, 61. (n) Yan, H.; Park, S. H.; Finkelstein, G.; Reif, J. H.; LaBean, T. H. *Science* **2003**, *30*, 1882. (o) Rinker, S.; Ke, Y.; Liu, Y.; Chhabra, R.; Yan, H. *Nat. Nanotechnol.* **2008**, *3*, 418. (p) Stephanopoulos, N.; Liu, M.; Tong, G. J.; Li, Z.; Liu, Y.; Yan, H.; Francis, M. B. *Nano Lett.* **2010**, *10*, 2714. (q) Voigt, N. V.; Tørring, T.; Rotaru, A.; Jacobsen, M. F.;

Ravnsbæk, J. B.; Subramani, R.; Mamdouh, W.; Kjems, J.; Mokhir, A.; Besenbacher, F.; Gothelf, K. V. *Nat. Nanotechnol.* **2010**, *5*, 200. (r) Liu, H.; Tørring, T.; Dong, M.; Rosen, C. B.; Besenbacher, F.; Gothelf, K. V. *J. Am. Chem. Soc.* **2010**, *132*, 18054. (s) Pinheiro, A. V.; Han, D.; Shih, W. M.; Yan, H. *Nat. Nanotechnol.* **2011**, *6*, 763. (t) Yan, H.; Yang, X.; Shen, Z.; Seeman, N. C. *Nature* **2002**, *415*, 62. (u) Zheng, J.; Birktoft, J. J.; Chen, Y.; Wang, T.; Sha, R.; Constantinou, P. E.; Ginell, S. L.; Mao, C.; Seeman, N. C. *Nature* **2009**, *461*, 74.

(8) (a) Dutta, P. K.; Varghese, R.; Nangreave, J.; Lin, S.; Yan, H.; Liu, Y. *J. Am. Chem. Soc.* **2011**, *133*, 11985. (b) Albinsson, B.; Hannestad, J. K.; Börjesson, K. *Coord. Chem. Rev.* **2012**, *256*, 2399. (c) Tong, A. K.; Jockusch, S.; Li, Z. M.; Zhu, H. R.; Akins, D. L.; Turro, N. J.; Ju, J. Y. *J. Am. Chem. Soc.* **2001**, *123*, 12923. (d) Hannestad, J. K.; Sandin, P.; Albinsson, B. *J. Am. Chem. Soc.* **2008**, *130*, 15889. (e) Stein, I. H.; Steinhauer, C.; Tinnefeld, P. *J. Am. Chem. Soc.* **2011**, *133*, 4193. (f) Börjesson, K.; Tumpane, J.; Ljungdahl, T.; Wilhelmsson, L. M.; Nordén, B.; Brown, T.; Mårtensson, J.; Albinsson, B. *J. Am. Chem. Soc.* **2009**, *131*, 2831. (g) Garo, F.; Häner, R. *Angew. Chem., Int. Ed.* **2012**, *51*, 916. (h) Kumar, C. V.; Duff, M. R., Jr. *J. Am. Chem. Soc.* **2009**, *131*, 16024. (i) Probst, M.; Langenegger, S. M.; Häner, R. *Chem. Commun.* **2014**, *50*, 159. (j) Woller, J. G.; Hannestad, J. K.; Albinsson, B. *J. Am. Chem. Soc.* **2013**, *135*, 2759. (k) Woller, J. G.; Borjesson, K.; Albinsson, B. *Biophys. J.* **2011**, *100*, 137. (l) Woller, J. G.; Hannestad, J. K.; Albinsson, B. *J. Am. Chem. Soc.* **2013**, *135*, 2759.

(9) (a) Milano, F.; Tangorra, R. R.; Omar, O. H.; Ragni, R.; Operamolla, A.; Agostiano, A.; Farinola, G. M.; Trotta, M. *Angew. Chem., Int. Ed.* **2012**, *51*, 11019. (b) Dutta, P. K.; Lin, S.; Loskutov, A.; Levenberg, S.; Jun, D.; Saer, R.; Beatty, J. T.; Liu, Y.; Yan, H.; Woodbury, N. W. *J. Am. Chem. Soc.* **2014**, *136*, 4599.

(10) Koepke, J.; Krammer, E. M.; Klingen, A. R.; Sebban, P.; Ullmann, G. M.; Fritzsch, G. *J. Mol. Biol.* **2007**, *371*, 396.

(11) (a) Allen, J. P.; Feher, G.; Yeates, T. O.; Komiya, H.; Rees, D. C. *Proc. Natl. Acad. Sci. U. S. A.* **1987**, *84*, 6162. (b) Feher, G.; Allen, J. P.; Okamura, M. Y.; Rees, D. C. *Nature* **1989**, *339*, 111. (c) Jones, M. R. *Prog. Lipid Res.* **2007**, *46*, 56.

(12) (a) Kirmaier, C.; Holten, D. *Photosynth. Res.* **1987**, *13*, 225. (b) Woodbury, N. W.; Allen, J. P. The Pathway, Kinetics and Thermodynamics of Electron Transfer in the Reaction Centers of Purple Nonsulfer Bacteria. In *Anoxygenic Photosynthetic Bacteria*; Blankenship, R. E., Madigan, M., Bauer, C. E., Eds.; Kluwer Academic Publishers: Dordrecht, The Netherlands, 1995; p 527. (c) Kirmaier, C.; Laporte, L.; Schenck, C. C.; Holten, D. *J. Phys. Chem.* **1995**, *99*, 8903. (d) Zinth, W.; Wachtveitl, J. *ChemPhysChem* **2005**, *6*, 871. (e) Parson, W. W.; Warchel. A. Mechanism of Charge Separation in Purple Bacterial Reaction Centers. In *The Purple Phototrophic Bacteria*; Hunter, C. N., Daldal, F., Thurnauer, M. C., Beatty, J. T., Eds.; Springer: Dordrecht, The Netherlands, 2009; p 355.

(13) Mahmoudzadeh, A.; Saer, R.; Jun, D.; Mirvakili, S. M.; Takshi, A.; Iranpour, B.; Ouellet, E.; Lagally, E. T.; Madden, J. D. W.; Beatty, J. T. *Smart Mater. Struct.* **2011**, *20* (9), 094019.

(14) Okamura, M. Y.; Feher, G. *Annu. Rev. Biochem.* **1992**, *61*, 861.

(15) Spinazzi1, M.; Casarin, A.; Pertegato, V.; Salviati, L.; Angelini, C. *Nat. Protoc.* **2012**, *7*, 1235.

(16) Gerencsér, L.; Laczkó, G.; Maróti, P. *Biochemistry* **1999**, *38*, 16866.